Advanced Analysis Technology for New Material and Product Development

Hirokazu Sasaki[*1], *Hideo Nishikubo*[*1], *Shinsuke Nishida*[*1], *Satoshi Yamazaki*[*1], *Ryusuke Nakasaki*[*2], *Takemi Isomatsu*[*2], *Ryuichiro Minato*[*3], *Kohei Kinugawa*[*3], *Akihiro Imamura*[*3], *Shinya Otomo*[*4], *Yujin Hori*[*5], *Kiyoshige Hirose*[*6], *Satoshi Anada*[*7], *Kazuo Yamamoto*[*7], *Tsukasa Hirayama*[*7], *Jun Yamasaki*[*8], *Naoya Shibata*[*9], *Yojiro Oba*[*10], *Masato Ohnuma*[*11]

ABSTRACT Several cases using advanced analysis technology including electron microscope, synchrotron radiation, and surface analysis for various new materials/products are introduced. Electron holography and the Differential Phase Contrast-Scanning Transmission Electron Microscopy (DPC-STEM) were used for the analysis of a semiconductor laser diode for optical communication. 3D analysis with Focused Ion Beam-Scanning Electron Microscopy (FIB-SEM) was utilized for analyzing winding wire with a micro cellular coating. The Small Angle X-ray Scattering (SAXS) method was used at Super Photon-ring-8-GeV (SPring-8) for analyzing a coated superconductor tape and a copper alloy. The surface analysis method of Hard X-ray Photoelectron Spectroscopy (HAXPES) was utilized for analyzing the AuSn solder.

1. INTRODUCTION

Furukawa Electric (FEC) offers a wide variety of products and fosters next-generation business based on the core technologies of photonics, polymers, metals, and high-frequency electronics. Examples in the photonics field include optical fibers, products related to the semiconductor laser diode etc. In the field of polymer technology application, various products include the tapes for semiconductors as well as various foamed products. In the metal field, typical products include copper alloys, oxygen-free copper, and aluminum blanking material for memory disks.

At the actual sites where new products are developed, it is important to have a thorough understanding of the materials that define the products. The relevant characteristics can be obtained by properly understanding compound semiconductors (GaAs, InP, etc.) in the case of the semiconductor laser diode, copper and aluminum in the case of metal products, and the adhesive compound in the case of the tape used for semiconductors.

In order to understand each material, the Analysis Technology Center at FEC has been analyzing the materials for the products manufactured in the plants and under development by using various analytical equipment. An overview of the roles undertaken of the Analysis Technology Center is provided in Figure 1. In the case of products currently under development, the elucidation of the mechanism behind the function expression and the characteristics of the new materials is carried out and then utilized as design guidelines for the new products. Also, when any type of problem occurs at the plant, we investigate the cause immediately from the viewpoint of material analysis and facilitate the problem solving.

[*1] Advanced Technologies R&D Laboratories, R&D Division
[*2] Automotive Products & Electronics Laboratories, R&D Division
[*3] Furukawa Fitel Optical Device Co.,Ltd
[*4] Corprate Planning Department, Strategy Division
[*5] HR Departmet, Strategy Division
[*6] Marketing Relationship Management Department, Marketing Initiatives & Business Development Department, Global Marketing Sales Division
[*7] Japan Fine Ceramics Center
[*8] Osaka University
[*9] The University of Tokyo
[*10] Japan Atomic Energy Agency
[*11] Hokkaido University

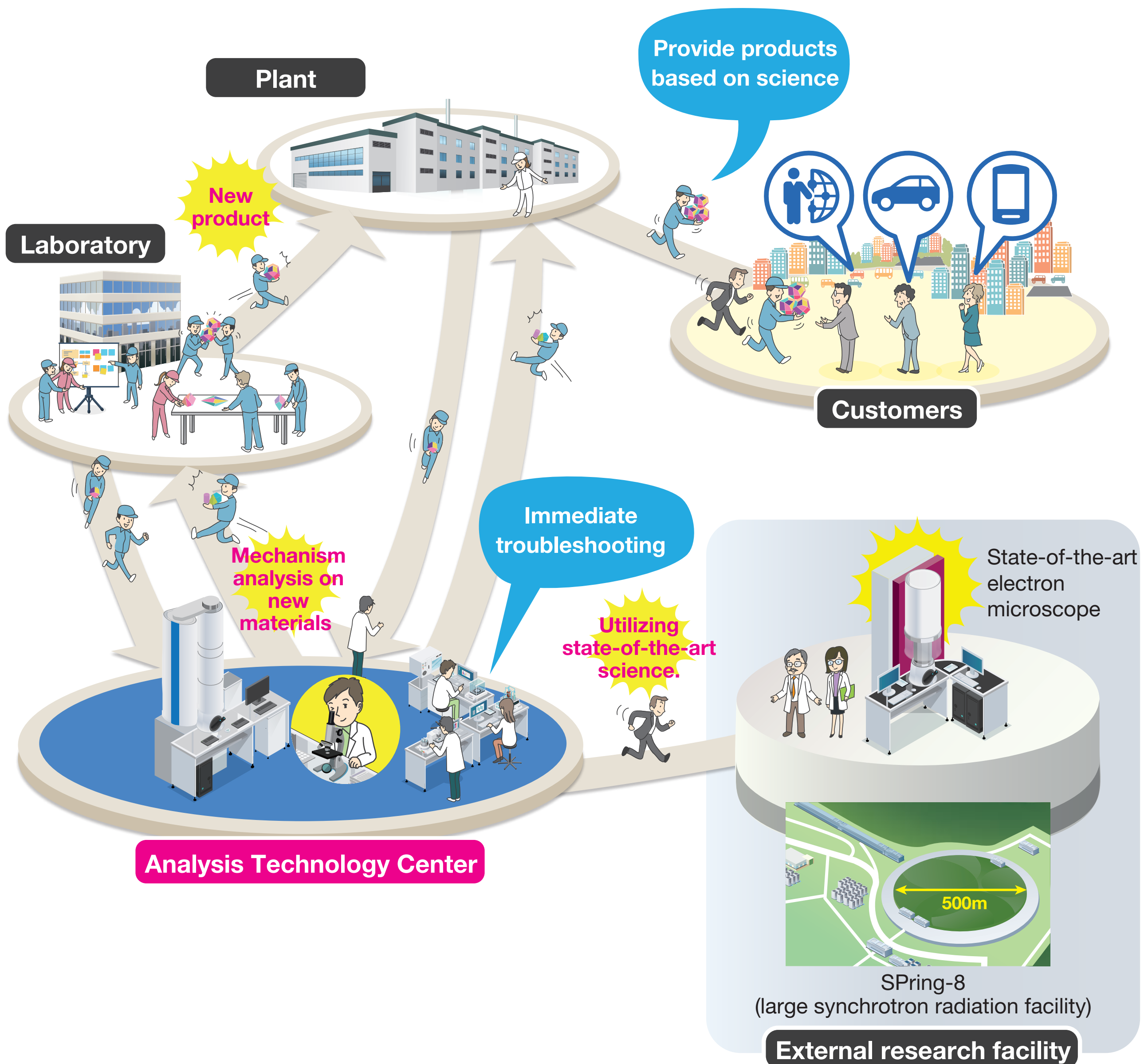

Figure 1 Roles of the analysis technology center.

In recent years, advanced analysis equipment has become more expensive, and it is often impractical to own every single piece of equipment that is needed. When our equipment is not sufficient for an analysis, we typically borrow an advanced electron microscope from a university or a synchrotron radiation facility such as Super Photon-ring-8-GeV (SPring-8). An important objective of the Analysis Technology Center is to provide customers with products based on science through reliable material analysis. To this end, we collaborate with universities and public research institutes that possess advanced analysis equipment and technology.

Thus far, we have applied advanced material analysis technology to the development of new materials and products by collaborating with many research institutes. The semiconductor analyses by electron holography and DPC-STEM discussed in this paper are collaborative projects with the Japan Fine Ceramics Center (JFCC) and the University of Tokyo, respectively. We carried out precise analysis of the p-n junction in collaboration with Osaka University. Our analyses of copper alloy and coated superconductor tape by SAXS utilizing SPring-8 are the results of research with Hokkaido University, the Japan Atomic Energy Agency, and Kyoto University.

Today, research facilities and analytical devices in universities and public institutions are well organized for private companies to use, and we utilize a lot of equipment to analyze various materials. We have used mainly SPring-8 and the Aichi Synchrotron Radiation Center for analysis by synchrotron radiation. We have also worked with the Japan Proton Accelerator Research Complex (J-PARC) for analysis using neutrons. For advanced electron microscopy and surface analysis, equipment owned by JFCC, the University of Tokyo, and Nagoya University is regularly utilized. In this paper, we introduce some application examples using advanced analysis technologies to analyze a number of new materials and products.

2. NEW PRODUCT ANALYSIS USING ELECTRON MICROSCOPY

An electron microscope is used to observe products by enlarging the view from several thousands to several million times by means of electron beams with a wavelength shorter than light. It is possible to observe the surface of a specimen with Scanning Electron Microscopy (SEM) and the inside of a specimen at a high magnification with Transmission Electron Microscopy (TEM). Which one to use is selected according to the purpose.

In this paper, electron holography and the DPC-STEM method are introduced as case studies of TEM, and as an example of SEM, a case of 3D analysis with Focused Ion Beam (FIB) is introduced.

2.1 Precise Analysis of Semiconductor p-n Junction by Electron Holography

As one method of TEM, the use of electron holography to observe the potential in a semiconductor initially proceeded as research with Si semiconductors.[1)-3)] In order to apply this technique to compound semiconductors, a joint research between JFCC and FEC was set up and successful observations with GaAs and InP were performed in 2006.[4)] More recently, it is being applied to the observation of devices such as semiconductor laser diodes.[5)] At the beginning of this research, the observation was mostly with the magnification of several thousands to tens of thousands of times. The resolution in the conventional electron holography was insufficient to observe the electric potential distribution of the semiconductor at a higher magnification, so we applied the phase-shifting method based on a double-biprism electron holography. In doing so, we have achieved high-resolution potential distribution observation on the p-n junction of GaAs.

A phase image with the electron holography is shown in Figure 2. The specimen was GaAs and the dopant concentration of the p-type semiconductor and the n-type semiconductor was 1×10^{19} cm^{-3} for each. From this dopant concentration, approximately 20 nm of the depletion layer width was expected. Using TEM (Hitachi HF-3300 EH; owned by JFCC), observation was conducted under the double-biprism condition, and the phase was reconstructed with the phase-shifting method. As shown in the phase image in Figure 2(a), the contrast difference clearly appears in the p-n junction. Regarding the area enclosed by the frame, the phase profile was created as shown in Figure 2(b). The potential distribution estimated from the dopant concentration is shown on the same graph. Since these two profiles are in close agreement, we can see that, by using electron holography, the potential change in the p-n junction with a 20-nm-wide depletion layer can be observed in the high spatial resolution.

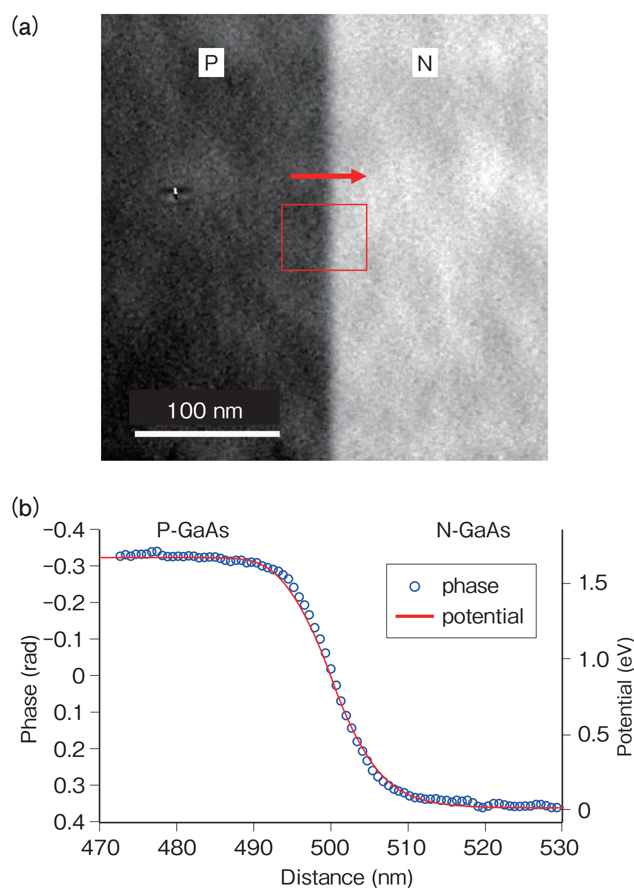

Figure 2 Precise analysis of the GaAs p-n junction with phase-shifting electron holography. (a) Phase image and (b) phase profile across the p-n junction.

On the basis of this result, we attempted to observe how the electric potential and the electric field change by applying a voltage to the p-n junction. In this experiment, electrodes with low contact resistance were formed on the surface of the semiconductor. We utilized the manufacturing process of the semiconductor laser diode in FEC for the electrode manufacturing.

The analysis results of the electric field profile are shown in Figure 3 (a). The applied voltage was varied from –0.3 to 0.5 V, and we successfully detected the associated changes in the electric field profile at the p-n junction. In addition, we were able to observe the depletion layer width caused by the voltage change. These results are in close alignment with the theoretical expectation, indicating that the experiment was properly performed.[6)] Thus, by using electron holography, the electric potential and the electric field can be directly visualized in high special resolution of several nm, and as such, it can be used for the development of new semiconductor devices.

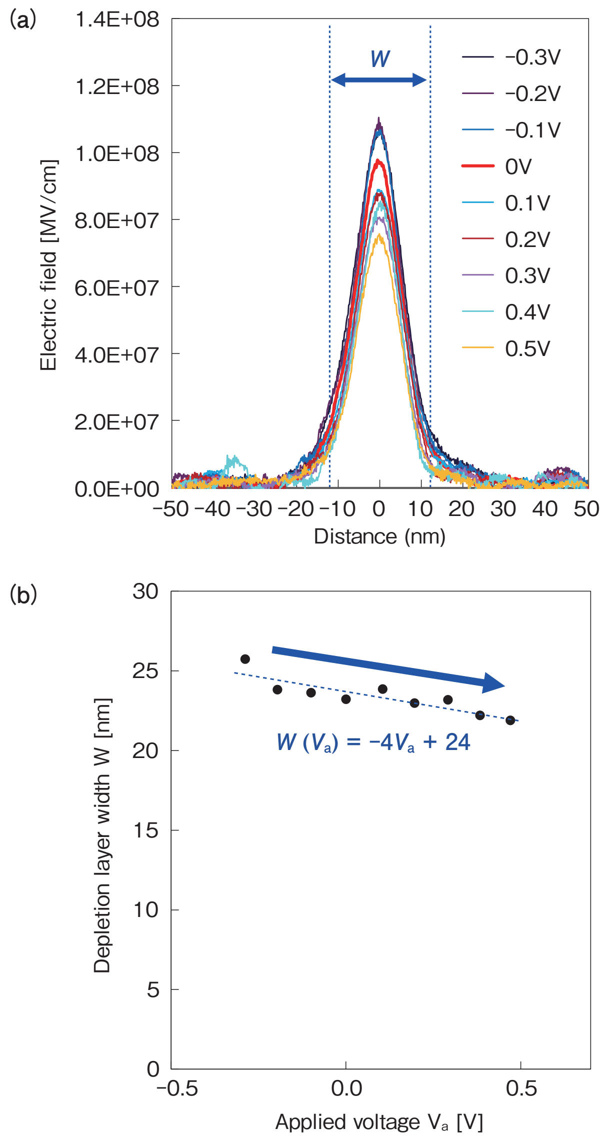

Figure 3 Precise measurement of electric field across GaAs p-n junction by in situ biasing and electron holography.
(a) Change in electric field profiles and (b) depletion layer width across p-n junctions.

2.2 Analysis of Semiconductor Laser Diode by Differential Phase Contrast (DPC) Method

Thanks to advancements with STEM, the electron beam can now be focused to the utmost limit, and atomic visualization is becoming a routine analysis. The DPC method, which is a method of STEM, has also shown significant progress in atomic resolution observation.[7] The University of Tokyo and FEC collaborated to observe the GaAs p-n junction in order to evaluate the electric field in semiconductors with DPC-STEM. With the cooperation of JEOL Ltd., we found the optimal observation condition for the p-n junction and succeeded in observing it.[8] Today, DPC-STEM is becoming a common method.

Figure 4 (a) shows the DPC-STEM image of a GaAs p-n junction. The JEOL 2100F TEM equipped with an aberration corrector (owned by the University of Tokyo) was used. The camera length was 140 m and the beam diameter was 12 nm. We found that the p-n junction could be clearly observed at the center of the DPC-STEM image. The arrows in the figure indicate the interfaces where the dopant concentrations changed, and as shown, even small potential changes could be observed.

With this method, devices having a 2D shape can be observed. A part of the semiconductor laser diode for the optical communication is shown in Figure 4. In the figure, (b) shows the image captured by the Annual Dark Field (ADF)-STEM method, which is a conventional method. In this image, the interface between the p-type semiconductor and the n-type semiconductor cannot be observed. In contrast, in the observation result by DPC-STEM, shown in (c), the 2D p-n junction that could not be observed in the ADF-STEM image is clearly visible. In this example, the device under observation was a characteristically defective item; specifically, the p-n junction shape was not as designed.[5] Thus, through the p-n junction observation using DPC-STEM, defects in products can be identified.

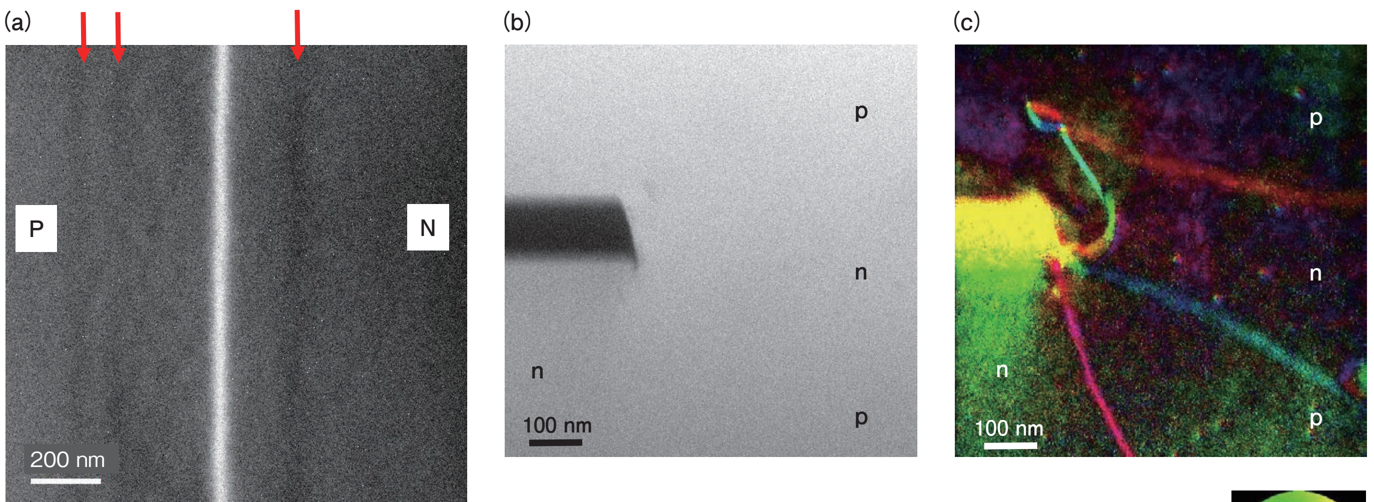

Figure 4 Observation by DPC-STEM on p-n junction and semiconductor laser diode.
(a) DPC-STEM image of the p-n junction region in GaAs. (b) ADF-STEM and (c) DPC-STEM image of the semiconductor laser diode.

In addition to the DPC-STEM and electron holography introduced thus far, semiconductor observation technology with the electron microscope has also been progressing. Research on electron diffractive imaging[9), 10)], 4D-STEM[11)], the shadow method[12)], etc. as new potential and electric field observation methods is currently underway. If we take advantage of these methods in a complementary way, further detailed progress in device analysis will become possible.

2.3 3D Analysis of Winding Wire with Micro Cellular Coating by FIB-SEM

Typical 3D analysis methods on the micron order or less include X-ray tomography, 3D analysis using FIB-SEM, TEM tomography, and the 3D atom probe method. The observable size of a specimen and its spatial resolution are different from each other, so it is necessary to select a suitable method for the purpose of the observed material. In this section, we introduce 3D structural analysis using FIB-SEM for the enamel part of the enameled winding wire containing micro-sized bubbles.

The winding wire with micro cellular coating can improve the partial discharge inception voltage by controlling the volume ratio and the size of the bubbles, and it contributes to the size reduction and the increase of the motor output.[13)] To ascertain the shape distribution of the bubbles, 3D images were taken using FIB and SEM. FIB can process the cross section at a high accuracy on the nm order with the focused ion beam, and furthermore, by irradiating the ion beams repeatedly to the processed cross section, a new cross section can be prepared. Utilizing this feature, as shown in Figure 5(a), by periodically repeating the cross section preparation with FIB and SEM observation, the 3D information of the material can be obtained.

When bubbles come into contact with each other, they are sometimes separated by walls thinner than 0.1 μm. Therefore, in the observation of bubbles containing enamel, the performance of the electron microscope mounted on the FIB-SEM is important. We therefore used an orthogonal type FIB-SEM (MI4000L; owned by Nagoya University), and instrument in which the FIB and SEM columns are orthogonally arranged. Since orthogonal FIB-SEM can keep the field of view almost completely steady, even when 500 or more section images are taken, it is possible to obtain 3D images with a wider range in the depth direction. The mounted SEM has a spatial resolution of 10 nm or less even under the observation condition of the low acceleration voltage of 3 keV or less, which is a sufficient performance for observing bubbles containing enamel.

An example of the SEM image is shown in Figure 5(b). The bubble size is several μm and bubbles with various shapes and sizes can be observed. However, observation from a single cross-section cannot provide information on the depth direction, which means that accurate structural information cannot be obtained. Therefore, in order to perform 3D observation, the section processing was performed using the FIB at 100-nm pitch, and 500 sheets of SEM images were obtained. The luminance information, which was obtained from the serial cross-sectional SEM images in the range of 50μm with respect to the depth direction, was converted into 3D pixels called voxels. This resulted in the 3D image shown in Figure 5 (c), complete with a visible 3D bubble shape formation.

By utilizing this 3D analysis method, the partial discharge inception voltage can be improved and the innovation of motor technology will thus be possible.

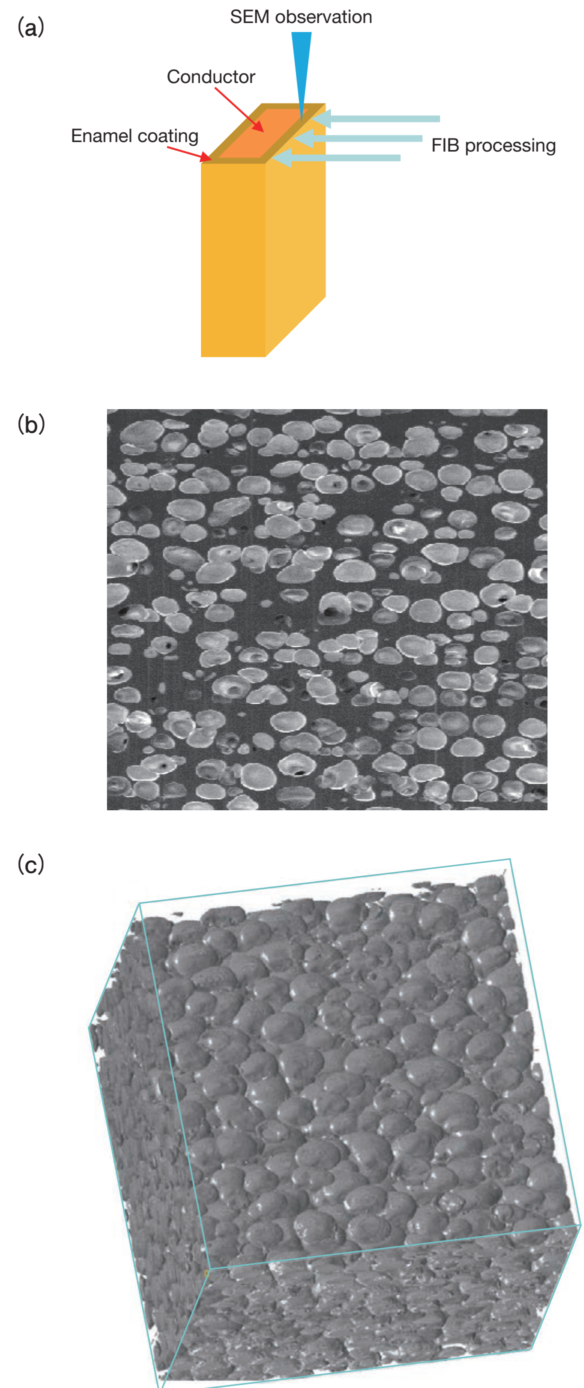

Figure 5 FIB-SEM 3D analysis of winding wires with micro cellular coating.
(a) Schematic diagram of FIB-SEM analysis (b) Cross section SEM image and (c) 3D reconstruction of the micro cellular coating.

3. PRODUCT ANALYSIS USING SYNCHROTRON RADIATION

Synchrotron radiation is a powerful electromagnetic wave emitted by charged particles accelerated to nearly the speed of light, with features including high brilliance, polarization, parallelism, pulsed light emission, and energy selectivity. Utilizing these characteristics of light, time-resolved measurement and X-ray absorption fine structure spectroscopy using X-rays near the absorption edge of a specific element are utilized in material analysis.

In this paper, we introduce cases of anomalous small-angle X-ray scattering (ASAXS), time-resolved SAXS measurement, and HAXPES utilizing these features.

3.1 Analysis of Artificial Pin in Superconducting Material by ASAXS Method

Since superconducting material has zero electric resistance at ultralow temperatures, it can contribute to a power saving environment due to its low electric power loss. It is also expected to be applied in products such as high voltage cables. In order to develop a tape with a high critical current density (Jc), control of the flux quantum is necessary. When the superconductor tape turns into a coil shape and is used as a strong magnetic field generator, a strong magnetic field is applied to the tape. When it is applied to the superconductor material, flux quantum is formed. With the current flow, the flux quantum moves with the Lorentz force, generating heat, and hence resistance is created. Therefore, it is necessary to pin the flux quantum into an appropriate normal conducting layer. Since around 2004, the development of an artificial pin to artificially introduce the pinning site into the superconducting material has been pursued.[14), 15)] One promising example is a rod-like normal conducting part with a diameter of several nm in the vertical direction of the thin layer that is formed as an artificial pin.[16)] If this artificial pin can be introduced as designed, the superconducting state can be maintained even in a high magnetic field, and a strong magnetic field then be generated.

In light of this background, material analysis on whether or not the artificial pins can be created as designed is necessary. For the artificial pin, although the analysis method for observation using TEM (as shown in Figure 6 (a)) is common, the observation area is as narrow as several μm, which is insufficient for the quantitative evaluation of size and distribution through the entire tape. Therefore, in order to establish a highly accurate quantitative evaluation method, we performed a nano-rod artificial pin evaluation using the small-angle scattering method.

In small-angle scattering, X-rays or neutrons are irradiated to materials and those that scatter at a small angle of 10 degrees or less are analyzed to obtain average information of the microstructures. Specifically, information on the average size and orientation of the nanoparticles and the secondary phase contained in the materials is obtained. It is effective for the material analysis to be used in conjunction with the TEM.

For artificial pins including heavy atoms such as Au, SAXS is applied as the artificial pin for the superconductor tape.[17)] However, the X-ray contrast of the practical $BaZrO_3$ in (Gd, Y) BaCuO is low due to the small difference of electron density from (Gd, Y) BaCuO of the superconductor phase, and sufficient scattering intensity cannot be obtained. Therefore, we aimed to establish a quantitative evaluation method of the size and dispersion state of the artificial pins using ASAXS targeting Zr. ASAXS targets anomalous X-ray scattering phenomena occurring in the energy region near the absorption edge of a specific element, and it is possible to change the scattering contrast in the small angle scattering measurement.

For the ASAXS measurement, we used a SAXS device installed in BL19B2 at SPring-8. Figure 6 (b) shows the anomalous small-angle X-ray scattering results of $(Gd, Y)_1Ba_2Cu_3O_7$ thin film in which 25% of Zr has been added. Profiles 1–4 in Figure 6 (b) show the measurement results at 17.885, 17.985, 17.990, and 17.995 keV, respectively. The Zr-K absorption edge is 17.998 keV. A shoulder was observed in the vicinity of q = 0.2–1.0 nm^{-1} (indicated by the arrow in (b)), and we confirmed the formation of a nano structure of several nm in the superconductor phase. Compared with profile 1, which was sufficiently far away from the absorption edge, peak intensities around q = 0.3 nm^{-1} increased for profiles 2, 3, and 4. These results suggest that the scattering of these peaks was caused by the artificial pins due to $BaZrO_3$ containing Zr.

The measurement results of the specimens with Zr addition amounts of 7.5%, 15%, 20%, and 25% are shown in Figure 6 (c). Using these results, the rod diameter was estimated with the unified fit.[18), 19)] As shown in Figure 6 (d), although the diameter tended to increase as the Zr concentration increased, there was no significant difference between the 20% and 25% specimens. Thus, by utilizing ASAXS, it is possible to analyze the artificial pins in the superconductor phase with a high accuracy, thus contributing to the development of superconductor wire with high critical current density.

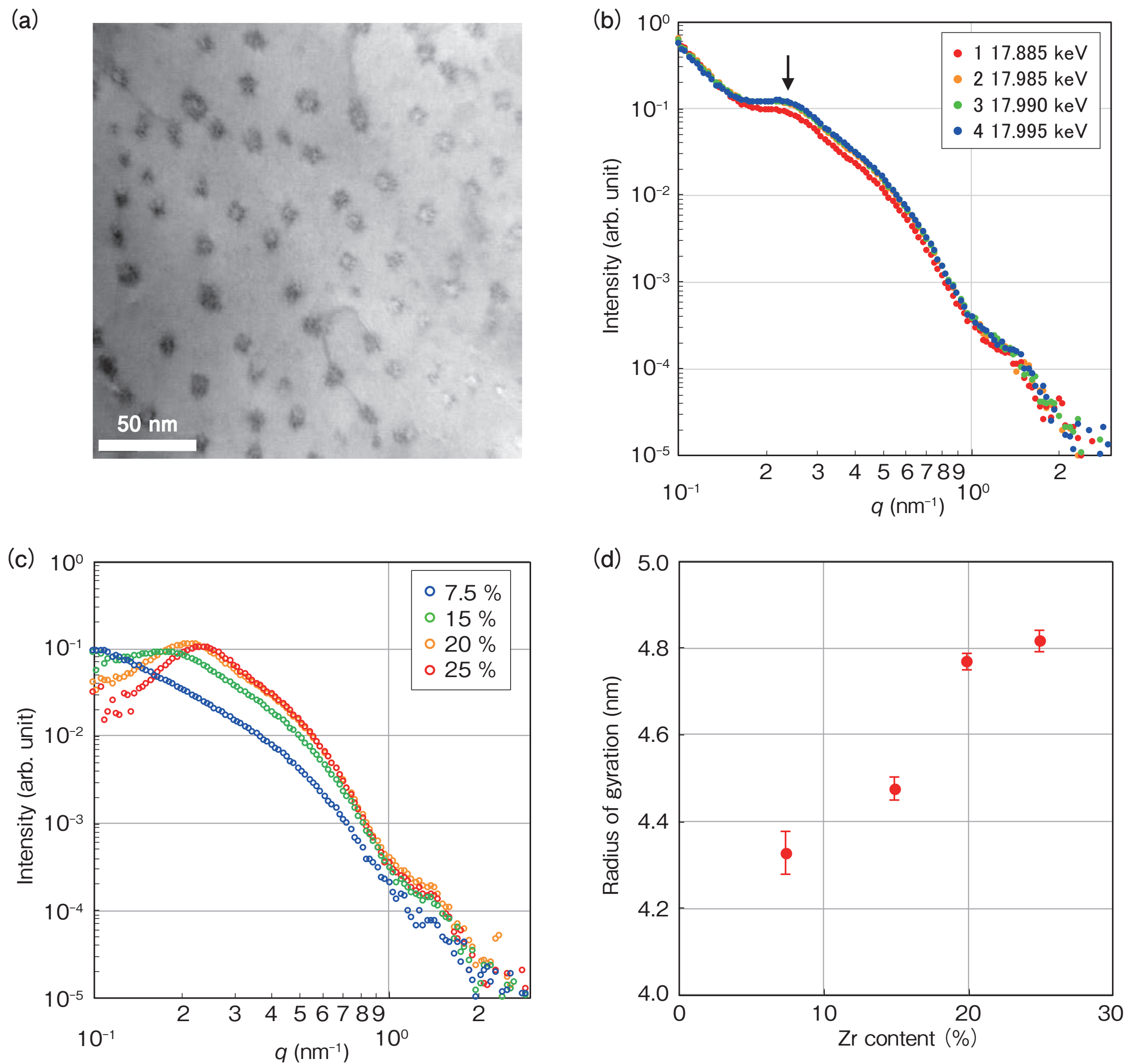

Figure 6 Characterization of artificial pin in the superconductor tape by ASAXS.
(a) TEM image of artificial pinning center (b) Energy dependence of the scattering profiles of Zr-added samples. (c) Anomalous small-angle X-ray scattering profiles and (d) average diameter of artificial pinning center in 25, 20, 15, and 7.5 mol% Zr-added samples.

3.2 In-situ Measurement of Cu-Ni-Si Precipitates by Small-Angle X-ray Scattering

Recently, along with the miniaturization and weight reduction of electric devices such as portable devices and personal computers, the electronic parts used for them are also becoming more miniaturized and their performances need to be improved. The performance required for the copper alloys used in, for example, the conducting parts of connectors is also increasing. In order to prevent insufficient terminal strength and insufficient conductivity due to the miniaturization of the terminals, materials with higher strength and higher conductivity than their conventional counterparts are required. Cu-Ni-Si alloys can satisfy these requirements, and as the TEM image in Figure 7 (a) shows, the strength can be improved by finely dispersing the Ni-Si based compound as a precipitate into the Cu parent phase by heat treatment. In order to clarify what strengthens the precipitation, quantitative evaluations of the precipitates on the size distribution and on the dispersion state are necessary. However, TEM observation is restricted to local information and is thus insufficient. Therefore, in order to obtain size information of the precipitates of Corson alloy and information on their growth process, in-situ SAXS measurement, which can obtain average information, was carried out.

For this SAXS measurement, the SAXS device installed at BL19B2 was used. We selected the x-ray energy of 18 keV, and a 2D position sensitive detector (PILATUS-2M) was used as a detector. For the aging treatment, the HS1300g heating stage by Instec Ltd. was used. The heating rate was set to 10°C/min. and the maximum attained temperature was 500°C.

Figure 7 (b) shows the profile during heating. During the temperature rise process, the shoulder changed to the low-q side, and the precipitates coarsened. (c) shows the profile change during isothermal holding time at aging temperature 500°C. As time goes by, the scattering intensity increased and the shoulder shifted to the low-q side. After four hours had elapsed, the profile did not appear saturated, and it tended to increase further and to shift to

the low-q side. By proceeding with such data analysis in detail, the mechanism behind the nucleation and grain growth can be clarified, which will be of great benefit in the development of new copper alloys.

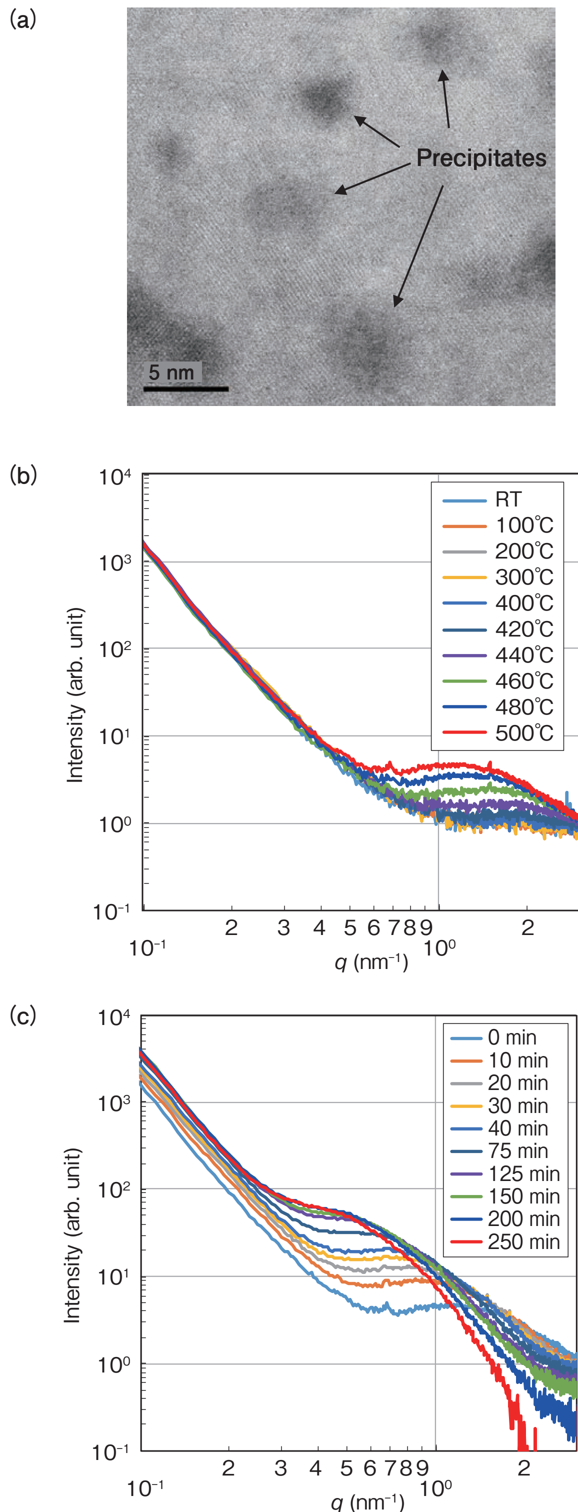

Figure 7 Measurement of Cu - Ni - Si alloy precipitates size by in-situ SAXS.
(a) TEM image (b) profile change during heating (c) profile change during isothermal holding time at 500 degrees.

3.3 AuSn Solder Oxide Film Analysis by HAXPES

X-ray Photoelectron Spectroscopy (XPS) is a surface analysis method used to obtain information on the element species, the composition, and the chemical state on the surface through the detection of photoelectrons emitted by irradiating a solid surface with X-rays. Since the surface state of the components used in products contributes greatly to the bonding characteristics between the components, it is very important to analyze the organic contamination layer, the thickness, and the chemical state of the oxide layer on the surface of the specimen.

Changes in oxide layer thickness can be evaluated from depth profiling analysis using Ar ion spattering. However, the chemical state and the electronic state of the sputtered surface are damaged by the sputtered ions, and there is a possibility that the original chemical state and the original electronic state of the material to be analyzed may be altered. In addition, since depth profiling analysis using ion spattering is a destructive analysis, in the case of only one specimen (such as a defective or faulty product), it is very difficult to perform the same or another analysis again.

We therefore use Hard X-ray Photoelectron Spectroscopy (HAXPES), which offers greater sampling depth of analysis compared to conventional XPS, so as to perform the oxide layer thickness evaluation and depth profiling analysis nondestructively. Over the past ten years, HAXPES experimentation utilizing the synchrotron radiation at SPring-8 is readily available for corporate R&D and products development[20)-22)], and FEC has also been conducting HAXPES measurement on BL46XU.

In this section, we report the analysis results for the AuSn solder used for jointing members in various products. The specimen used for the analysis were two types of AuSn solder (specimens A and B) with different Sn oxide layer thickness. The oxide layer thicknesses obtained from the depth profiling analysis by XPS were ca. 2 nm for specimen A and ca. 11 nm for specimen B.

Figure 8(a) shows the Sn3d spectrum obtained by measuring the surfaces of specimens A and B with XPS. The XPS instrument we used was a Refurbished ESCA5400MC (by Physical Electronics Inc.) owned by FEC. The incident X-ray was the monochromatic Al Kα (1486.6 eV) and the take-off-angle was 75°. In specimen A, two components of Sn oxide film layer and AuSn were detected, but only the Sn oxide layer component was detected in specimen B, and the underlying AuSn component was not detected.

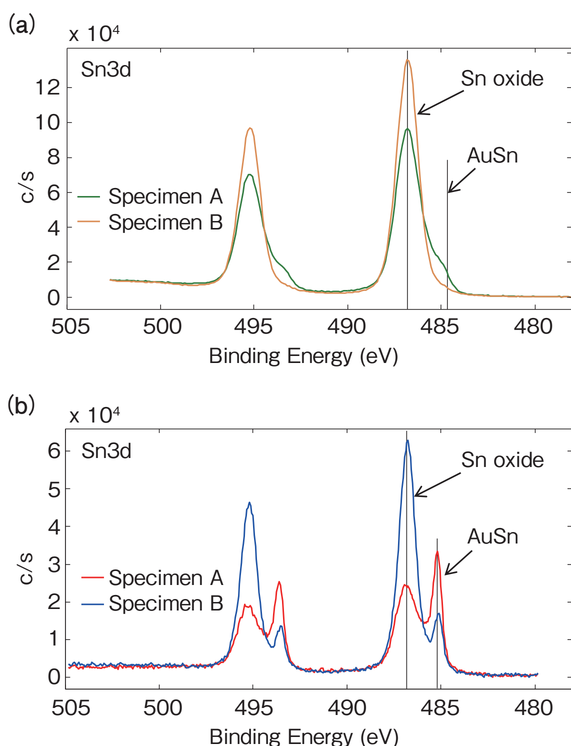

Figure 8 Oxide film analysis of the AuSn solder surface by (a) XPS and (b) HAXPES.

The Sn3d spectrum obtained by measuring AuSn solder specimens A and B with HAXPES is shown in Figure 8(b). The HAXPES measurement was performed using BL46XU at SPring-8. The incident X-ray energy was 7939.0 eV and the take-off-angle was 80°. In the HAXPES measurement, two components of the Sn oxide layer and AuSn were detected not only in specimen A but also in specimen B, in which only the Sn oxide layer was detected by XPS measurement. This means that nondestructive thickness evaluation, chemical state analysis, and depth of analysis profiling analysis of the Sn oxide layer on AuSn solder is possible with HAXPES due to its greater sampling depth. By applying this technique, we are able to clarify the component bonding mechanism used in various products.

4. CONCLUSION

As discussed in this paper, by utilizing various advanced analysis equipment and analysis technology in the field of new material/new products development, we can obtain information that is vital in determining the design guidelines. In addition, even in existing products, the advanced analysis technology may play an important role in some cases. We will continue to develop new analytical technologies in order to provide highly reliable products that are embraced by society.

ACKNOWLEDGEMENTS

A part of this work was supported by the project for promoting public utilization of advanced research infrastructure and the Advanced Characterization Nanotechnology Platform of the University of Tokyo, and as well by Nagoya University through the Nanotechnology Platform of the Ministry of Education, Culture, Sports, Science and Technology (MEXT), Japan. A part of this work was supported by JSPS KAKENHI Grant Numbers JP26286049 and JP26600042. The synchrotron radiation experiments were performed at SPring-8 with the approval of the Japan Synchrotron Radiation Research Institute (JASRI) (Proposal Nos. 2016B1790, 2014A1814, 2014B1942, 2015B1789, 2017B1803, and 2018B1655). A variety of state-of the-art research facilities and support systems have been developed to clarify technical issues in the industry, and we wish to thank and express our sincere gratitude to the people concerned for the great benefits this has provided our research.

REFERENCES

1) M. R. McCartney, D. J. Smith, R. Hull, J. C. Bean, E. Voelkl and B. Frost: “Direct observation of potential distribution across Si/Si p-n junctions using off-axis electron holography”, Appl.Phys. Lett., 65 (1994), 2603.
2) W. D. Rau, P. Schwander, F. H. Baumann, W. Höppner, and A. Ourmazd: “Two-Dimensional Mapping of the Electrostatic Potential in Transistors by Electron Holography”, Phys. Rev.Lett., 82 (1999), 2614.
3) Z. Wang, T. Hirayama, K. Sasaki, H. Saka and N. Kato: “Electron holographic characterization of electrostatic potential distributions in a transistor sample fabricated by focused ion beam”, Appl. Phys. Lett., 80 (2002), 246.
4) H. Sasaki, K. Yamamoto, T. Hirayama, S. Ootomo, T. Matsuda, F. Iwase, R. Nakasaki and T. Ishii: “Mapping of dopant concentration in a GaAs semiconductor by off axis phaseshifting electron holography”, Appl. Phys. Lett., 89 (2006), 244101.
5) H. Sasaki, S. Otomo, R. Minato, J. Yoshida: “Analysis of The Semiconductor Laser Diode Using Off-axis Electron Holography and Lorentz Microscopy” Furukawa Review 46 (2015), 19.
6) S. Anada, K. Yamamoto, H. Sasaki, N. Shibata, Y. Hori, K. Kinugawa, A. Imamura and T. Hirayama: “Precise measurement of electric potential, field, and charge density profiles across a biased GaAs p-n tunnel junction by in situ phase-shifting electron holography”, Journal of Applied Physics, 122 (2017), 225702.
7) N. Shibata, S. D. Findlay, Y. Kohno, H. Sawada, Y. Kondo and Y. Ikuhara: “Differential phase-contrast microscopy at atomic resolution”, Nature Physics, 8 (2012), 611.

8) N. Shibata, S. D. Findlay, H. Sasaki, T. Matsumoto, H. Sawada, Y. Kohno, S. Otomo, R. Minato and Y. Ikuhara: “Imaging of built-in electric field at a p-n junction by scanning transmission electron microscopy”, Scientific Reports, 5 (2015), 10040.
9) J. Yamasaki, K. Ohta, S. Morishita and N. Tanaka: “Quantitative phase imaging of electron waves using selected-area diffraction” Appl. Phys. Lett., 101 (2012), 234105.
10) J. Yamasaki, K. Ohta, H. Sasaki and N. Tanaka: “Observation of electric field using electron diffractive imaging”, 18th International Microscopy Congress, Prague, (2014).
11) R. Sagawa, H. Hashiguchi, H. Sasaki, R. Ritz, M. Simson, M. Huth, G. T. Martinez, P. D. Nellist and Y. Kondo: “Development of fast pixelated STEM detector and its applications for visualization of electromagnetic field and ptychographic reconstruction using 4D dataset”, 19th International Microscopy Congress, Sydney, (2018).
12) K. Sasaki, H. Sasaki and S. Saito: “Differential Potential Distribution Observation in Transmission Electron Microscope with Conventional Thermal Electron Gun” Proceedings of Microscopy & Microanalysis 2018, 24 (Suppl 1), (2018), 26.
13) D. Muto, K. Ikeda, K. Tomizawa, H. Fukuda, M. Kozato, M. Hikita: “Partial Discharge Characteristics of Winding Wire Utilizing Micro Cellular Coating” Furukawa Review 50, (2019) .
14) J. L. M. Driscoll, S. R. Foltyn, Q. X. Jia, H. Wang, A. Serquis, L. Civale, B. Maiorov, M. Hawley, M. P. Maley and D. E. Peterson: “Strongly enhanced current densities in superconducting coated conductors of YBa2Cu3O7–x + BaZrO3”, Nature Materials, 3 (2004), 439.
15) Y. Yamada, K. Takahashi, H. Kobayashi, M. Konishi, T. Watanabe, A. Ibi, T. Muroga, S. Miyata, T. Kato, T. Hirayama and Y. Shiohara: “Epitaxial nanostructure and defects effective for pinning in Y„RE…Ba2Cu3O7−x coated conductors”, Appl. Phys. Lett. 87, (2005), 132502.
16) T. Kato, H. Sasaki, Y. Gotoh, Y. Sasaki, T. Hirayama, K. Takahashi, M. Konishi, H. Kobayashi, A. Ibi, T. Muroga, S. Miyata, T. Watanabe, Y. Yamada, T. Izumi and Y. Shiohara: “Nanostructural characterization of Y123 and Gd123 with BaZrO3 rods Fabricated by Pulsed-Laser Deposition” Physica C, 445-448, (2006), 628.
17) T. Horide, K. Matsumoto, H. Adachi, D. Takahara, K. Osamura, A. Ichinose, M. Mukaida, Y. Yoshida and S. Horii: “Evaluation of metallic nanoparticles in REBa2Cu3O7-δ (RE = Y, Gd) thin films by small angle X-ray scattering” , Physica C, 445-448, (2006), 652.
18) J. Ilavsky and P. R. Jemian: “Ultra-small-angle X-ray scattering at the Advanced Photon Source”, J. Appl. Cryst. 42, (2009) 347.
19) G. Beaucage: “Approximations Leading to a Unified Exponential Power-Law Approach to Small-Angle Scattering”, J. Appl. Cryst., 28 (1995), 717.
20) K. Kobayashi, Y. Takata, T. Yamamoto, J.-J. Kim, H. Makino, K. Tamasaku, M. Yabashi, D. Miwa, T. Ishikawa, S. Shin and T. Yao: “Intrinsic Valence Band Study of Molecular-Beam-Epitaxy-Grown GaAs and GaN by High-Resolution Hard X-ray Photoemission Spectroscopy”, Jpn. J. Appl. Phys., 43, (2004), L1029.
21) Y. Saito, M. Nakamura, A. Kimura, K. Yamaguchi and M. Ito: “Characterization of SiNx/GaxIn1-xAs Interface using Hard X-ray Photoemission Spectroscopy”, Jpn. J. Appl. Phys., 46, (2007), 5771.
22) T. Doi, K. Kitamura, Y. Nishiyama, N. Otsuka, T. Kudo, M. Sato, E. Ikenaga, K. Kobayashi and T. Hashimoto: “Analysis of Cu segregation to oxide-metal interface of Ni-base alloy by HX-PES”, Surf. Interface Anal., 40, (2008), 329.